

PREDICTION OF WAVE FORCE ACTING ON HORIZONTAL PLATE ABOVE STILL WATER LEVEL

Susumu Araki¹ and Ichiro Deguchi²

The applicability of the existing prediction methods to estimating the wave force acting on a horizontal plate above the still water level is investigated by comparing the estimated wave force with the measured wave force. The applicability of a numerical model as well as the equations from experimental results is also investigated. Some prediction methods overestimate the measured wave force, and some prediction methods underestimate the measured wave force.

Keywords: wave force; wave pressure; horizontal plate; bridge

INTRODUCTION

The huge tsunami which struck the northeastern coasts of Japan on March 11, 2011 caused a catastrophic damage to the coastal zones. In the area which the tsunami struck, many bridges as well as houses were washed away. The blockade of roads brought about the delay in the transportation of relief and the reconstruction of the area.

The tsunami wave force acting on bridges has not been taken into account in the present design in Japan. Therefore, the stability and the countermeasures of bridges against tsunamis have to be investigated. Many studies on fluid force acting on coastal and harbor structures have been conducted. Cross (1967) investigated the impact forces acting on vertical walls. Goda (1974) proposed the formula for estimating the design wave pressure acting on a caisson of composite breakwaters. Ramsden and Raichlen (1990) measured the fluid force and pressure due to bore. Asakura *et al.* (2002) measured the fluid force acting on structures on the land by a tsunami overflowing seawalls. Arnason *et al.* (2009) measured the fluid force acting on vertical columns due to bore and the water surface and the velocity in detail. Nouri *et al.* (2010) measured the fluid force and pressure due to bore acting on both cylindrical and square structures placed on a dry bed. Several studies on tsunami fluid force acting on bridge beams which have clearance under them have been conducted since Indian Ocean Tsunami in 2004. Shoji and Moriyama (2007) investigated the characteristics of the wave force acting on a bridge and the stability of the bridge. The characteristics of the wave force acting on bridge beams are partly similar to that acting on pier deck, which have been investigated by many researchers, *e.g.*, Tanimoto *et al.* (1978), Kaplan and Silbert (1976), Suchithra and Koola (1995) and Cuomo *et al.* (2007).

The authors have investigated the characteristics of wave force acting on bridges measured in experiments (Araki and Deguchi, 2009; Araki *et al.* 2010; Araki and Deguchi, 2011). The aim of this study is to investigate the prediction methods of the wave force acting on a horizontal plate. The applicability of the methods for predicting the wave pressures and the wave forces proposed by Goda (1974) and Cuomo *et al.* (2007) are investigated. The applicability of a numerical model in which the wave pressure is computed is also investigated.

HYDRAULIC EXPERIMENT

The hydraulic experiments were conducted in a wave flume which is 43.0 m long and 0.7 m wide in Osaka University. Figure 1 shows a rough sketch of the experimental set-up. The wooden horizontal plate was installed above the 1/40 bottom slope. The incident wave like a solitary wave was generated by piston type wave generator. Figure 2 shows a definition sketch of the parameters. η_{max} is the maximum rise in the water surface in front of the horizontal plate, d is the water depth at the horizontal plate and c_l is the clearance under the horizontal plate. F_x and F_z are the horizontal and vertical components of the wave force acting on the horizontal plate. The horizontal and vertical fluid forces acting on the horizontal plate were measured by strain gauges on a cantilever-type force measuring device made with aluminum. The wave pressure at eight points P1 – P8 on the horizontal plate shown in Figure 3 was measured by pressure gauges. The measured data were digitized at the time interval of 0.001 s (1000 Hz) and were recorded by a data acquisition system. In this experiment, the incident wave did not break in front of the horizontal plate in almost all of the experimental runs. There is one

¹ Dept. of Civil Engineering, Osaka University, 2-1 Yamada-oka, Suita, Osaka, 565-0871, Japan

² NEWJEC Inc., 2-3-20 Honjo-Higashi, Kita-ku, Osaka 531-0074, Japan

peak value in each of the measured time series because the incident wave like a solitary wave was used. The details of the hydraulic experiment are described by Araki and Deguchi (2011).

APPLICABILITY OF EQUATIONS PROPOSED BY CUOMO ET AL.

Impulsive and Quasi-static Wave Pressure

Figure 4 shows the ratio of the impulsive wave pressure p_{imp} to the quasi-static wave pressure p_{qst} acting on the underside of the horizontal plate. The vertical axis shows the ratio and the horizontal axis shows the maximum rise in the water surface above the horizontal plate normalized by the water depth d . The black circle, white circle and triangle show the ratios measured at P1, P2 and P3, respectively. Although the ratios are scattered, the ratio decreases with the increase in the maximum rise in the water surface above the horizontal plate. The quasi-static wave pressures are scattered. However, it seems that the scattering of the ratio mainly results from the scattering of the impulsive wave pressure. In almost all of the following sections, the estimated quasi-static wave pressures are compared with the measured quasi-static wave pressure.

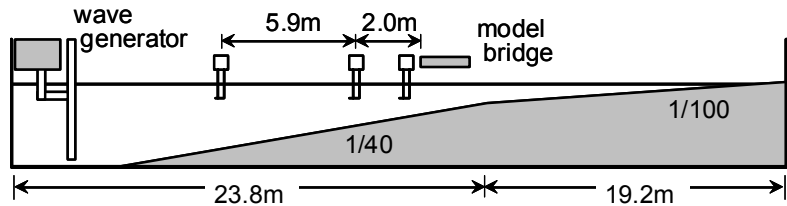


Figure 1. Experimental Set-up.

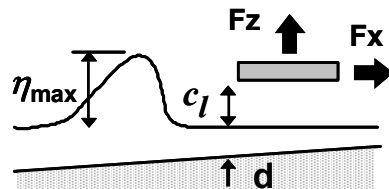


Figure 2. Definition sketch of parameters.

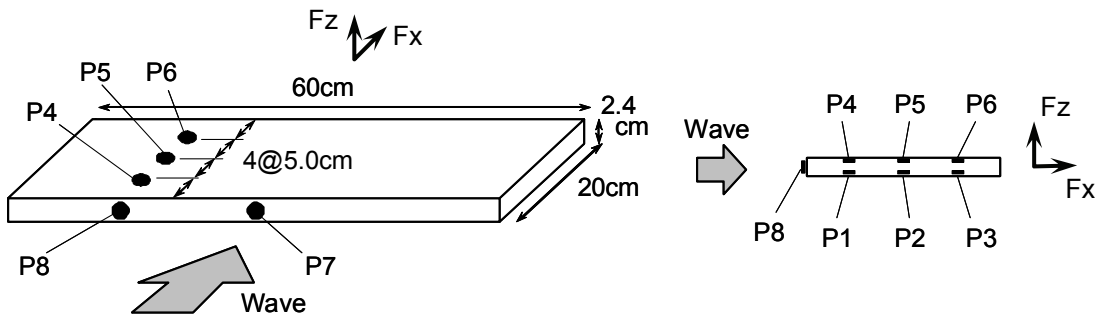


Figure 3. Horizontal plate and points where wave pressures are measured.

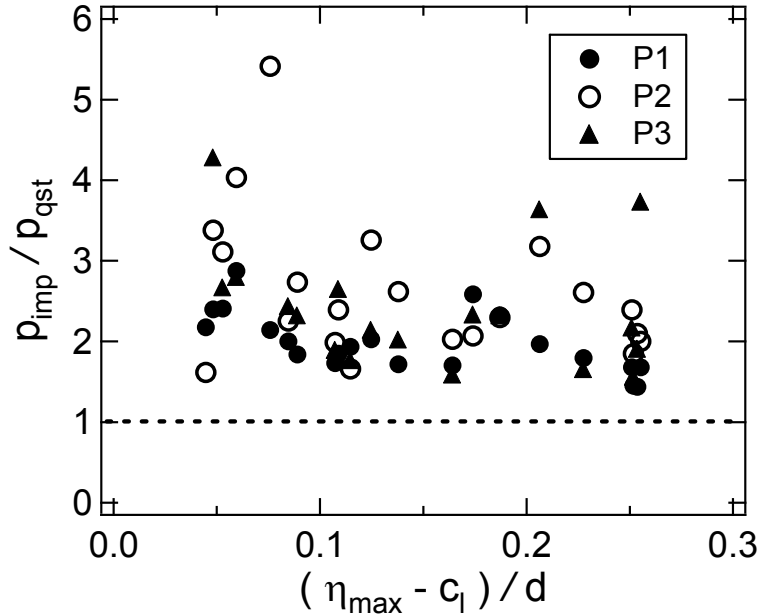


Figure 4. Ratio of impulsive wave pressure to quasi-static wave pressure.

Vertical Wave Force

The vertical wave force estimated by the equation proposed by Cuomo *et al.* (2007) was compared with the measured vertical wave force acting on the horizontal plate. Figure 5 shows the relationship between the quasi-static vertical wave force in the positive direction and the maximum rise in the water surface. The vertical axis shows the quasi-static positive vertical wave force normalized by the water density ρ , the gravitational acceleration g , the wave height in front of the horizontal plate H and the area of the horizontal plate on which the vertical wave force acts A (20cm×60cm). The horizontal axis shows the maximum rise in the water surface above the horizontal plate normalized by the water depth d . In the figure, the solid and the broken lines show the quasi-static vertical wave forces in the positive direction estimated by the equations for the external and the internal flat decks proposed by Cuomo *et al.* (2007), respectively. The equations for the external and the internal flat decks are as follows:

For the external flat deck:

$$\frac{Fz_{qs1/250}}{\rho \cdot g \cdot H_s \cdot A} = 2.31 \cdot \left(\frac{\eta_{\max} - c_l}{d} \right) + 0.05 \quad (1)$$

For the internal flat deck:

$$\frac{Fz_{qs1/250}}{\rho \cdot g \cdot H_s \cdot A} = 0.83 \cdot \left(\frac{\eta_{\max} - c_l}{d} \right) + 0.13 \quad (2)$$

where $Fz_{qs1/250}$ is the quasi-static vertical wave force at 1/250 level and H_s is the significant wave height. In Eqs. (1) and (2), the quasi-static vertical wave force is normalized by the significant wave height H_s . On the contrary, the measured quasi-static vertical wave force in Figure 5 is normalized by not significant wave height but wave height of the incident wave like a solitary wave H .

The normalized quasi-static vertical wave force increases with the increase in the normalized maximum rise in the water surface in both of the measured and the estimated vertical wave forces. However, both of the equations for the external and the internal flat decks overestimate the measured positive quasi-static vertical wave force acting on the horizontal plate. The difference between the measured and the estimated wave forces may result from the normalization of the quasi-static vertical wave force by wave height. In Eqs. (1) and (2) proposed by Cuomo *et al.* (2007), the quasi-static vertical wave forces are normalized by the significant wave height H_s because the incident wave was irregular. On the contrary, the measured quasi-static vertical wave force is normalized by the wave

height of the wave like a solitary wave H . If the wave height in front of the horizontal plate H is assumed to be the maximum wave height in an irregular wave train, the wave height H is approximately 1.8 times larger than the significant wave height. Taking this into account, Eq. (2) for the internal flat deck almost estimates the upper limit of the measured quasi-static vertical wave force.

Figure 6 shows the relationship between the quasi-static vertical wave force in the negative direction and the maximum rise in the water surface. In the figure, the solid and the broken lines show the vertical wave forces in the negative direction estimated by the equations for the external and the internal flat decks proposed by Cuomo *et al.* (2007), respectively. The equations for the external and the internal flat decks are as follows:

For the external flat deck:

$$\frac{F_{z_{qs}}}{\rho \cdot g \cdot H_s \cdot A} = -1.95 \cdot \left(\frac{\eta_{max} - c_l}{d} \right) + 0.03 \quad (3)$$

For the internal flat deck:

$$\frac{F_{z_{qs}}}{\rho \cdot g \cdot H_s \cdot A} = -0.52 \cdot \left(\frac{\eta_{max} - c_l}{d} \right) - 0.05 \quad (4)$$

The normalized quasi-static vertical wave force decreases with the increase in the normalized maximum rise in the water surface in both of the measured and the estimated vertical wave forces. Although Eq. (3) for the external flat deck overestimates the absolute values of the measured quasi-static vertical wave forces in many conditions, Eq. (4) for the internal flat deck estimates the average of the measured quasi-static vertical wave force. Taking account of the relationship between the significant wave height H_s and the wave height of the incident wave like a solitary wave H , Eqs. (3) and (4) almost estimate the upper and lower limits of the absolute value of the measured quasi-static vertical wave force, respectively.

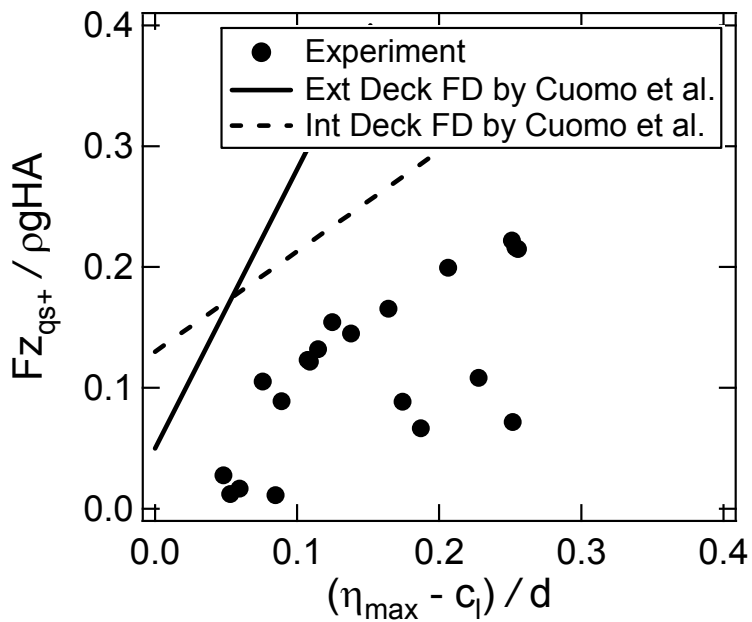


Figure 5. Quasi-static vertical wave force in positive direction.

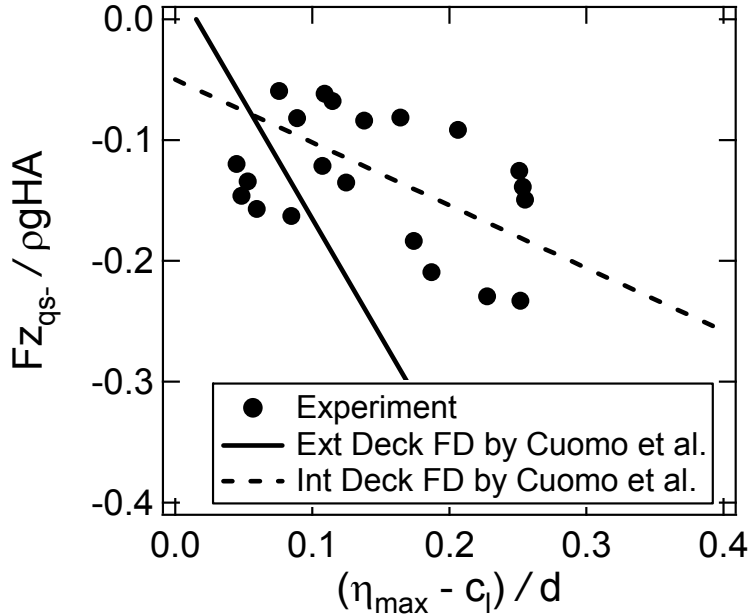


Figure 6. Quasi-static vertical wave force in negative direction.

Wave Pressure Acting on Seaward Side

The wave pressure acting on the seaward side of the horizontal plate estimated by the equation proposed by Cuomo *et al.* (2007) was compared with the wave pressure measured at P7 and P8. Figure 7 shows the relationship between the quasi-static wave pressure acting on the seaward side of the horizontal plate and the maximum rise in the water surface. The vertical axis shows the quasi-static wave pressure acting on the seaward side of the horizontal plate normalized by the water density ρ , the gravitational acceleration g and the wave height in front of the horizontal plate H . The horizontal axis shows the maximum rise in the water surface above the horizontal plate normalized by the water depth d . In the figure, the solid line shows the quasi-static wave pressure acting on the seaward side of the horizontal plate estimated by the equation proposed by Cuomo *et al.* (2007). The equation is as follows:

$$\frac{P_{qs,1/250}}{\rho \cdot g \cdot H_s} = 1.19 \cdot \left(\frac{\eta_{\max} - c_l}{d} \right) + 0.43 \quad (5)$$

In Eq. (5), the quasi-static wave pressure is normalized by the significant wave height H_s . On the contrary, the measured quasi-static wave pressure measured in Figure 7 is normalized by not significant wave height but wave height of the incident wave like a solitary wave H .

Although the normalized quasi-static vertical wave pressures acting on the seaward side of the horizontal plate are scattering, they increase with the increase in the maximum rise in the water surface. Eq. (5) estimates the average of the measured quasi-static wave pressure. Taking account of the relationship between the significant wave height H_s and the wave height in the wave like a solitary wave H , Eq. (5) approximately estimates the lower limit of the measured quasi-static wave pressure.

Wave Pressure Acting on Underside

Figure 8 shows the relationship between the quasi-static wave pressures acting on the underside of the horizontal plate measured at P1, P2 and P3 and the maximum rise in the water surface. The vertical axis shows the quasi-static wave pressure acting on the underside of the horizontal plate normalized by ρ , g and H . The horizontal axis shows the maximum rise in the water surface above the horizontal plate normalized by the water depth d . The black circle, white circle and triangle show the normalized quasi-static wave pressures measured at P1, P2 and P3, respectively. The solid line in the figure shows the equation from the regression analysis of all the wave pressures measured at P1, P2 and P3 because Cuomo *et al.* (2007) did not measure the wave pressure acting on the underside of the deck.

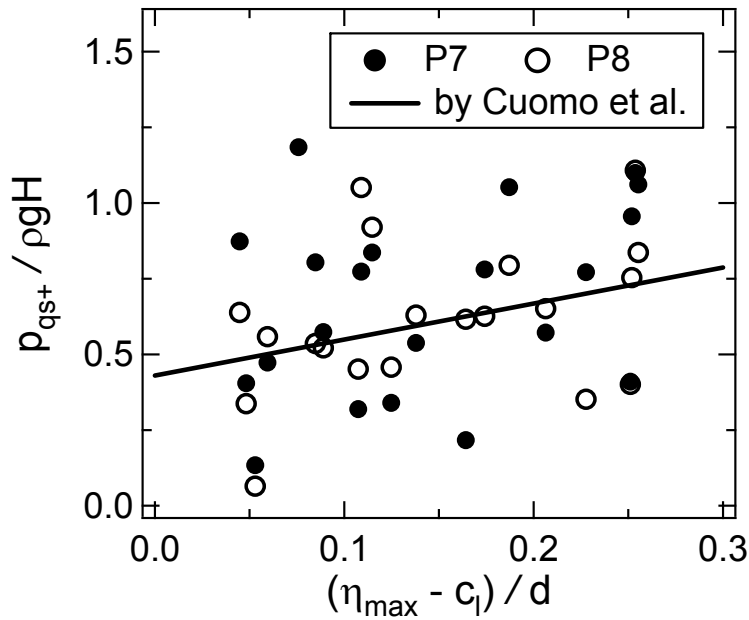


Figure 7. Quasi-static wave pressure acting on seaward side.

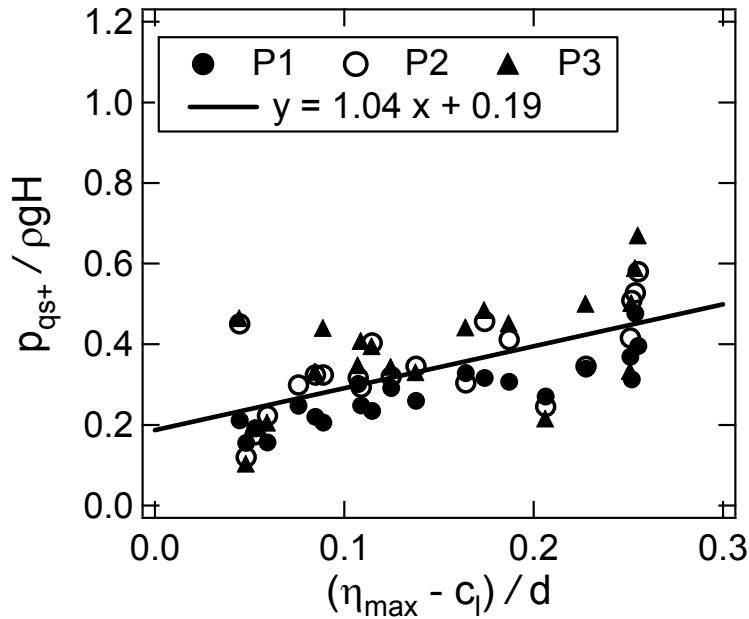


Figure 8. Quasi-static wave pressure acting on underside.

The quasi-static wave pressure acting on the underside of the horizontal plate increases with the increase in the maximum rise in the water surface. The quasi-static wave pressures measured at P2 were slightly larger than those measured at P1 in many cases. The quasi-static wave pressures measured at P3 were slightly larger than those measured at P2 in many cases.

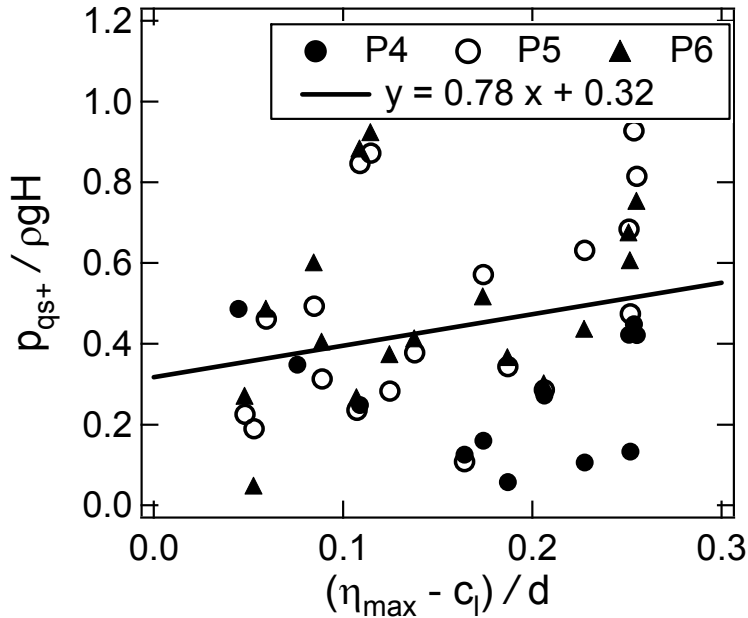


Figure 9. Quasi-static wave pressure acting on upper side.

Wave Pressure Acting on Upper Side

Figure 9 shows the relationship between the quasi-static wave pressures acting on the upper side of the horizontal plate measured at P4, P5 and P6 and the maximum rise in the water surface. The vertical axis shows the quasi-static wave pressure acting on the upper side of the horizontal plate normalized by ρ , g and H . The horizontal axis shows the maximum rise in the water surface above the horizontal plate normalized by the water depth d . The black circle, white circle and triangle show the normalized quasi-static wave pressures measured at P4, P5 and P6, respectively. The solid line in the figure shows the equation from the regression analysis of all the wave pressures measured at P4, P5 and P6 because Cuomo *et al.* (2007) did not measure the wave pressure acting on the upper side of the deck as well as the underside of the deck.

The quasi-static wave pressure acting on the upper side of the horizontal plate increases with the increase in the maximum rise in the water surface. The quasi-static wave pressures acting on the upper side of the horizontal plate are scattering. In several cases, the measured quasi-static wave pressures are approximately two times larger than the equation from the regression analysis. In several cases, the measured quasi-static wave pressures are less than half of the equation.

APPLICABILITY OF GODA'S FORMULA

Goda (1974) proposed the formula for the wave pressure acting on upright sections of composite breakwaters against high waves. Goda's formula has been widely used for designing composite breakwaters. The formula is originally not applied to the estimation of the wave pressure acting on horizontal plates with clearance between the structures and the water surface, such as deck structures and bridge beams. However, the applicability of the formula to the estimation of the quasi-static wave pressure acting on the horizontal plate was investigated.

In Goda's formula, the influence of the wave period is included. The equation for the wave pressure against tsunami is derived by making the wave period close to the infinity. A set of the equations for the wave pressure against tsunami is as follows (The Overseas Coastal Area Development Institute of Japan, 2009):

$$\eta^* = 3.0a_t \quad (6)$$

$$p_t = 2.2\rho_0 g a_t \quad (7)$$

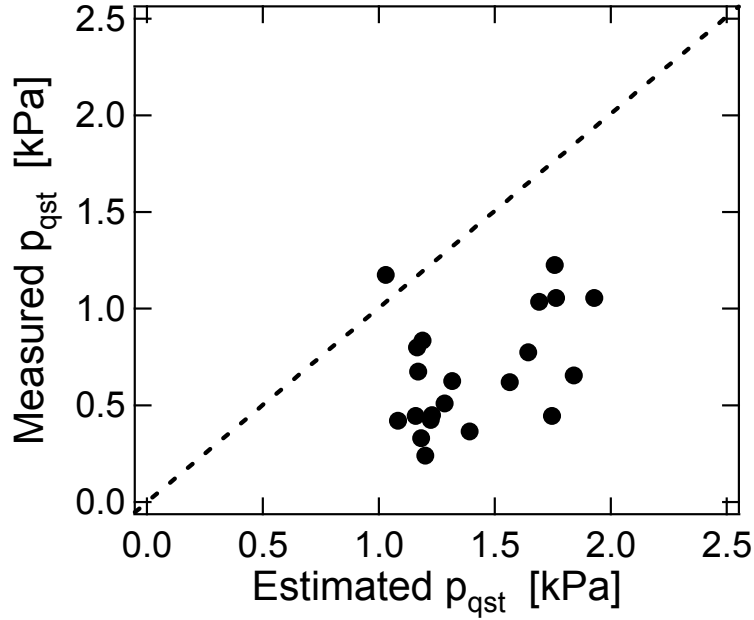


Figure 10. Quasi-static wave pressure acting on underside.

$$p_u = p_1 \quad (8)$$

where η^* is the wave pressure acting height above the still water surface, a_l is the incident tsunami height, ρ_0 is the density of the seawater, p_1 is the wave pressure at the still water surface and p_u is the uplift pressure at the lower edge of the front surface.

In the experiment, the incident wave was like a solitary wave. Therefore, the applicability of the equations for tsunami wave pressure derived from Goda's formula (Eqs. (6)–(8)) to the estimation of the quasi-static wave pressure acting on the seaward side of the horizontal plate was investigated.

Figure 10 shows the comparison between the quasi-static wave pressures acting on the seaward side of the horizontal plate measured in the experiments and estimated by Eqs. (6)–(8). The vertical and the horizontal axes show the quasi-static wave pressures measured in the experiment and estimated by Eqs. (6)–(8), respectively. In the set of Eqs. (6)–(8), the wave pressure distribution acting on upright sections of composite breakwaters is triangular above the still water level and is uniform below the still water level. In the triangular wave pressure distribution above the still water level, the wave pressure at the height equivalent to the horizontal plate in the experiment was assumed to be the wave pressure estimated by Eqs. (6)–(8). The equations overestimate the measured quasi-static wave pressure except one condition.

APPLICABILITY OF NUMERICAL MODEL

Numerical Model

The wave pressure and the wave force simulated with a numerical model were compared with the measured wave pressure and wave force. CADMAS-SURF in which the water surface is computed by VOF (Volume of Fluid) method (Isobe *et al.* 1999; Coastal Development Institute of Technology 2001) was used as a numerical model. The governing equations of this model are as follows:

The continuity equation:

$$\frac{\partial \gamma_x u}{\partial x} + \frac{\partial \gamma_z w}{\partial z} = S_p \quad (9)$$

The momentum equation:

$$\lambda_v \frac{\partial u}{\partial t} + \frac{\partial \lambda_x u u}{\partial x} + \frac{\partial \lambda_z w u}{\partial z} = -\frac{\gamma_v}{\rho} \frac{\partial p}{\partial x} + \frac{\partial}{\partial x} \left[\lambda_x v_e \left(2 \frac{\partial u}{\partial x} \right) \right] + \frac{\partial}{\partial z} \left[\gamma_z v_e \left(\frac{\partial u}{\partial z} + \frac{\partial w}{\partial x} \right) \right] + S_u - R_x \quad (10)$$

$$\lambda_v \frac{\partial w}{\partial t} + \frac{\partial \lambda_x u w}{\partial x} + \frac{\partial \lambda_z w w}{\partial z} = -\frac{\gamma_v}{\rho} \frac{\partial p}{\partial z} + \frac{\partial}{\partial x} \left[\gamma_x v_e \left(\frac{\partial w}{\partial x} + \frac{\partial u}{\partial z} \right) \right] + \frac{\partial}{\partial z} \left[\gamma_z v_e \left(2 \frac{\partial w}{\partial z} \right) \right] + S_w - R_z - \gamma_v g \quad (11)$$

where t is time, u and w are the horizontal and the vertical velocities, p is the pressure, ρ is the water density, v_e is the kinematic viscosity (sum of the molecular viscosity v and the eddy viscosity v_t), γ_v is the porosity, γ_x and γ_z are the horizontal and the vertical permeability and λ_v , λ_x and λ_z are expressed by γ , χ_x , χ_z , γ_z and the inertia coefficient C_M . S_p , S_u and S_w are the source terms for the wave generation. R_x and R_z are the resistance terms for porous structures.

Figure 11 show the computational domain, which is a part of the wave flume where the experiment was conducted. The boundary for generating incident waves was set at 8.0m offshore from the horizontal plate. The damping zone was set at the onshore end of the computational domain. There was no porous structure in the computational domain. The grid sizes Δx and Δz were 0.01m and 0.006m, respectively. In the numerical simulation, the incident wave was generated at the offshore boundary so that the maximum rise in the water surface in front of the horizontal plate was equal to that measured in the experiment.

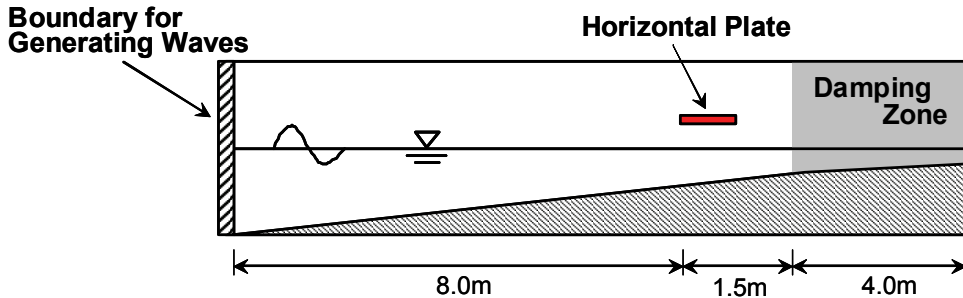


Figure 11. Computational domain.

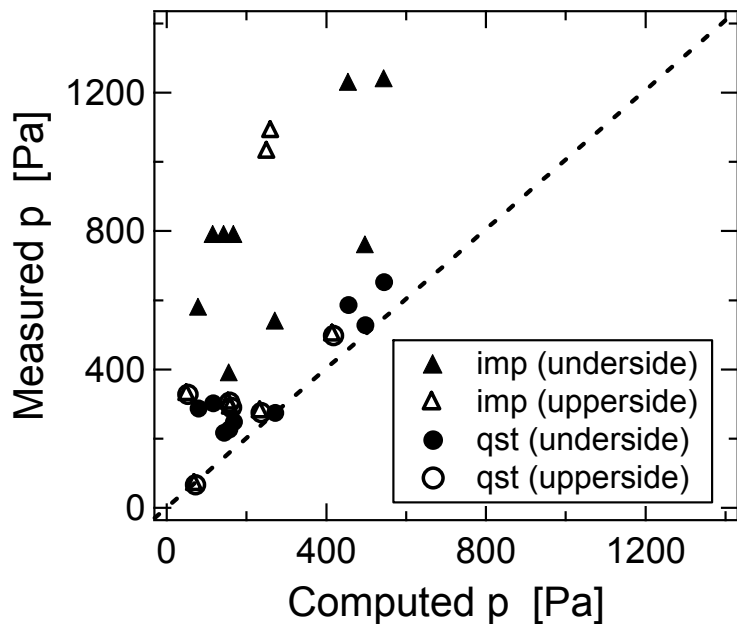


Figure 12. Comparison between measured and simulated wave pressures.

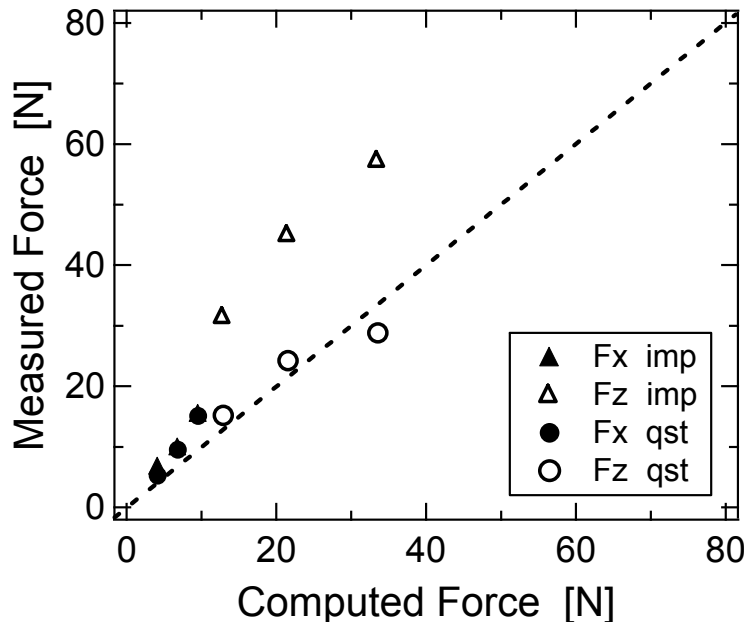


Figure 13. Comparison between measured and simulated wave forces.

Comparison between Measured and Simulated Wave Pressure and Wave Force

Figure 12 shows the comparison between the measured and the simulated wave pressures acting on the underside and the upper side of the horizontal plate. The vertical and the horizontal axes show the measured and the simulated wave pressures, respectively. The black and white triangles show the impulsive wave pressures acting on the underside and the upper side of the horizontal plate, respectively. The black and white circles show the quasi-static wave pressures acting on the underside and the upper side of the horizontal plate, respectively. The numerical model underestimates both impulsive and quasi-static wave pressures. Although the quasi-static wave pressures are slightly underestimated in many conditions, the simulated impulsive wave pressures in several cases are less than one third of the measured impulsive wave pressures.

Figure 13 shows the comparison between the measured and the simulated wave forces acting on the horizontal plate. The vertical and the horizontal axes show the measured and the simulated wave forces, respectively. The black and white triangles show the impulsive wave forces in the horizontal and vertical directions, respectively. The black and white circles show the quasi-static wave forces in the horizontal and vertical directions, respectively. The numerical model almost estimates the quasi-static wave forces in the horizontal and the vertical directions. However, it could not estimate the vertical impulsive wave force. In order to improve the accuracy of the numerical simulation, the details of the computational conditions need to be reconsidered. However, not only the computation of the water motion but also the computation of the air motion might be needed because the air between the water surface and the horizontal plate might have an influence on the wave pressure acting on the horizontal plate. CADMAS-SURF is a one-phase flow model.

CONCLUSIONS

In this study, the applicability of the prediction methods to estimating the wave force acting on the horizontal plate above the still water level was investigated. The wave forces or the wave pressures estimated by the equation proposed by Cuomo *et al.* (2007), Goda's formula (1974) and simulated with numerical model CADMAS-SURF were compared with the measured wave forces or wave pressures. The obtained results are summarized as follows:

- The equations proposed by Cuomo *et al.* (2007) overestimated the measured positive quasi-static wave force acting on the horizontal plate. The difference between the measured and the estimated wave forces may result from the normalization of the quasi-static vertical wave force by wave height. If the wave height for normalizing the quasi-static vertical wave force is selected properly, the equations for the internal flat deck proposed by Cuomo *et al.* (2007) almost estimated the upper limit of the measured quasi-static vertical wave force.
- The equations proposed by Cuomo *et al.* (2007) estimated the average of the measured quasi-static wave pressure acting on the seaward side of the horizontal plate. However, the attention needs to be paid to selecting the wave height for normalizing the quasi-static wave pressure.
- Goda's formula (1974) for designing upright sections of composite breakwaters overestimated the measured quasi-static wave pressure acting on the seaward side of the horizontal plate in most cases.
- The numerical model CADMAS-SURF underestimated both impulsive and quasi-static wave forces and wave pressures in most cases. Although the numerical model slightly underestimated the quasi-static wave force and wave pressure, it considerably underestimated the impulsive wave force and wave pressure. Although the details of the computational conditions need to be reconsidered, the computation of the air motion as well as the water motion might be needed.

REFERENCES

- Araki, S., and I. Deguchi. 2009. Experimental study on tsunami fluid force on bridge across narrow river, *Proceedings of 5th International Conference on Asian and Pacific Coasts*, Vol. 1, 143-150.
- Araki, S., K. Ishino, and I. Deguchi. 2010. Stability of girder bridge against tsunami fluid force, *Proceedings of 32nd International Conference on Coastal Engineering*, Paper #: structures.56. Retrieved from <http://journals.tdl.org/ICCE/>
- Araki, S. and I. Deguchi. 2011. Characteristics of wave pressure and fluid force acting on bridge beam by tsunami, *Proceedings of 6th Coastal Structures International Conference* (in press)
- Arnason, H., C. Petroff, and H. Yeh. 2009. Tsunami bore impingement onto a vertical column, *Journal of Disaster Research*, Vol. 4, No. 6, 391-403.
- Asakura, R., K. Iwase, T. Ikeya, M. Takao, T. Kaneto, N. Fujii, and M. Ohmori. 2002. The tsunami wave force acting on land structures, *Proceedings of 28th International Conference on Coastal Engineering*, 1191-1202.
- Coastal Development Institute of Technology. 2001. Research and development of a numerical wave flume; CADMAS-SURF, Report of the research group for development of numerical wave flume for the design of maritime structures, 296p (in Japanese).
- Cross, R. H. 1967. Tsunami surge forces, *Journal of Waterways and Harbor Division*, ASCE, Vol. 93, No. 4, 201-231.
- Cuomo, G., M. Tirindelli, and W. Allsop. 2007. Wave-in-deck loads on exposed jetties, *Coastal Engineering*, Vol. 54, 657-679.
- Goda, Y. 1974. New wave pressure formulae for composite breakwaters, *Proceedings of 14th International Conference on Coastal Engineering*, 1702-1720.
- Isobe, M., S. Takahashi, S. P. Yu, T. Sakakiyama, K. Fujima, K. Kawasaki, Q. Jiang, M. Akiyama, and H. Oyama. 1999. Interim development of a numerical wave flume for maritime structure design, *Proceeding of Civil Engineering in the Ocean*, Vol. 15, JSCE, 321-326 (in Japanese).
- Kaplan, P., and M. N. Silbert. 1976. Impact forces on platform horizontal members in the splash zone, *Proceedings of Offshore Technology*, 749-758.
- Nouri, Y., I. Nistor, and D. Palermo. 2010. Experimental investigation of tsunami impact on free standing structures, *Coastal Engineering Journal*, Vol. 52, No. 1, 43-70.
- Ramsden, J. D., and F. Raichlen. 1990. Forces on vertical wall caused by incident bores, *Journal of waterway, Port, Coastal, and Ocean Engineering*, ASCE, Vol. 116, No. 5, 592-613.
- Shoji, G., and T. Moriyama. 2007. Evaluation of the structural fragility of a bridge structure subjected to a tsunami wave load, *Journal of Natural Disaster Science*, Vol. 29, No. 2, 73-81.
- Suchithra, N., and P. M. Koola. 1995. A study of wave impact on horizontal slabs, *Ocean Engineering*, Vol. 22, No. 7, 687-697.
- Tanimoto, K., S. Takahashi, and Y. Izumida. 1978. A calculation method of uplift force on a horizontal platform, Report of Port and Harbour Research Institute, Vol. 17, No. 2, 3-47 (in Japanese).

The Overseas Coastal Area Development Institute of Japan. 2009. Technical standards and commentaries for port and harbour facilities in Japan, 998p.